Photochemical & Photobiological Sciences

Accepted Manuscript

This is an *Accepted Manuscript*, which has been through the Royal Society of Chemistry peer review process and has been accepted for publication.

Accepted Manuscripts are published online shortly after acceptance, before technical editing, formatting and proof reading. Using this free service, authors can make their results available to the community, in citable form, before we publish the edited article. We will replace this *Accepted Manuscript* with the edited and formatted *Advance Article* as soon as it is available.

You can find more information about *Accepted Manuscripts* in the Information for Authors.

Please note that technical editing may introduce minor changes to the text and/or graphics, which may alter content. The journal's standard Terms & Conditions and the Ethical guidelines still apply. In no event shall the Royal Society of Chemistry be held responsible for any errors or omissions in this *Accepted Manuscript* or any consequences arising from the use of any information it contains.

ROYAL SOCIETY OF CHEMISTRY

www.rsc.org/pps

Journal Name

RSCPublishing

ARTICLE

Assembly of photosynthetic reaction center with ABA tri-block polymersomes: highlights on the protein localization.

Cite this: DOI: 10.1039/x0xx00000x

Received 00th January 2012,
Accepted 00th January 2012

DOI: 10.1039/x0xx00000x

www.rsc.org/

R. R. Tangorra,[a] A. Operamolla,[a] F. Milano,[b] O. Hassan Omar,[c] J. Henrard,[d] R. Comparelli,[b] F. Italiano,[b] A. Agostiano,[a,b] V. De Leo,[a] R. Marotta,[e] A. Falqui,[f] G. M. Farinola,[a,c*] and M. Trotta[b*]

The reconstitution of the integral membrane protein photosynthetic reaction center (RC) in polymersomes, *i. e.* artificial closed vesicles, was achieved by the micelle-to-vesicle transition technique, a very mild protocol based on size exclusion chromatography often used to drive the incorporation of proteins contemporarily to liposomes formation. An optimized protocol was used to successfully reconstitute the protein in a fully active state in polymersomes formed by the tri-block copolymers $PMOXA_{22}$-$PDMS_{61}$-$PMOXA_{22}$. The RC is very sensitive to its solubilizing environment and was used to probe the positioning of the protein in the vesicles. According to charge-recombination experiments and to the enzymatic activity assay, the RC is found to accommodate in the $PMOXA_{22}$ region of the polymersome, facing the water bulk solution, rather than in the $PDMS_{61}$ transmembrane-like region. Furthermore, polymersomes were found to preserve protein integrity efficiently as the biomimetic lipid bilayers but show a much longer temporal stability than lipid based vesicles.

Introduction

Biological membranes play several roles, but arguably the most important is to form a boundary that separates the inside solution of cells or organelles from the outside milieu. Within the membrane sits the complex molecular machinery on which regulation, communication and translocation between the separated compartments rely. Given the complexity of the biological membranes, the molecular machineries of interest have been reconstituted in numerous model biomimetic structures, to gain insights into their specific activities. These biomimetic systems are based either on lipids (membrane models)[1] or on ad hoc designed amphiphilic molecules (artificial membranes)[2] and can accommodate membrane proteins and enzymes. Under suitable conditions, membrane models organize in closed systems, ranging from liposomes to giant vesicles that have been reconstituted with a large variety of enzymes performing a plethora of transmembrane functions.[3] Membrane models are extremely versatile, but present drawbacks in terms of chemical stability and mechanical robustness.[4]

Artificial membranes, based on synthetic amphiphilic molecules able to self-assemble in water and possessing higher stability and robustness than lipids, have been investigated as possible alternative to reconstitute membrane proteins and investigate specific transmembrane processes.[5] In particular, block co-polymers have drawn attention since self-organize in closed vesicles (polymersomes) in which membrane proteins can be inserted. Channel proteins, such as Aquaporins,[6] bacterial receptor protein LamB[7], bacteriorhodopsin, ATP synthase[8], NADH:Ubiquinone Oxidoreductase respiratory complex I[9], to name a few, were successfully reconstituted into block copolymers polymersomes retaining full enzymatic activity. Preparation of polymersomes requires amphiphilic block copolymers having the appropriate balance between the hydrophobic and the hydrophilic portions of the chains. A class of tri-block copolymers largely used is composed of two external hydrophilic poly-(2-methyloxazoline) (PMOXA) blocks and a hydrophobic poly-(dimethylsiloxane) (PDMS) central core: $PMOXA_n$-$PDMS_m$-$PMOXA_n$, also shortened as $A_nB_mA_n$, with n and m being the number of monomeric units in the copolymer blocks.[10] Membrane protein reconstitution in ABA polymersomes, e.g. by insertion in preformed polymersomes, ethanol injection or solid rehydration, requires the optimization of each method according to the nature of the

biological macromolecule.[11, 12] The first attempt to produce polymersomes using a mild and protein-friendly procedure known as micelle-to-vesicle transition (MVT)[13], is recent.[14]

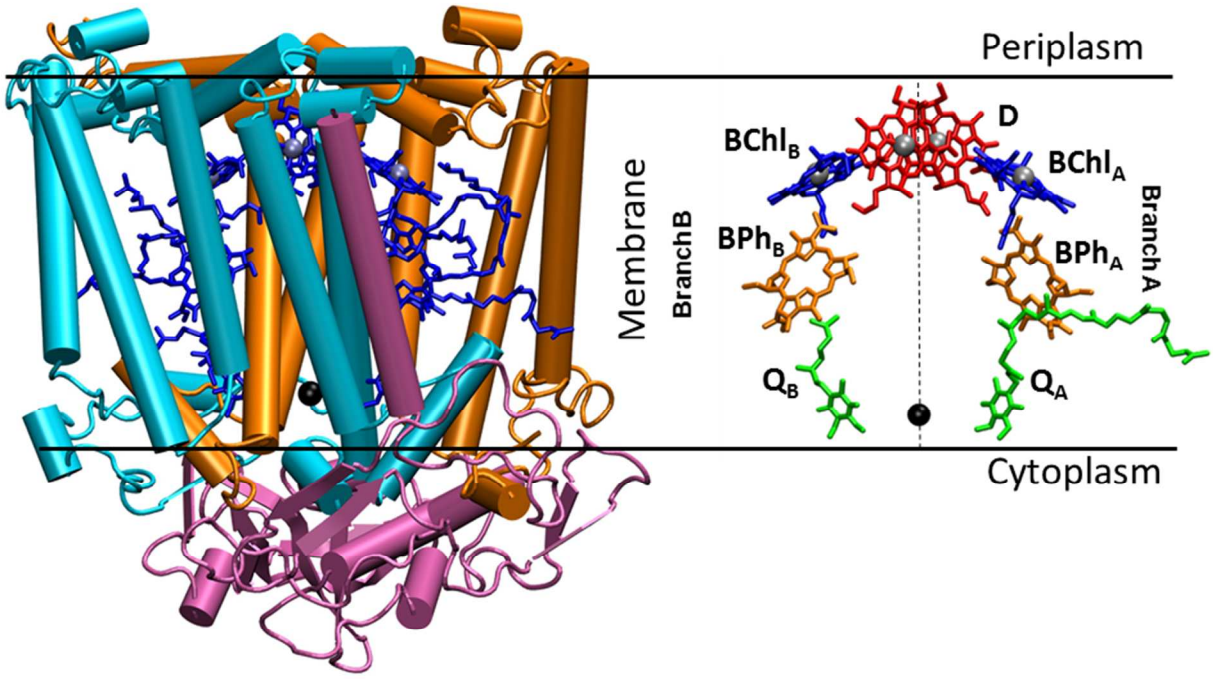

Figure 1. Reaction center of the photosynthetic bacterium *R. sphaeroides* R26 (PDB entry: 2J8C[15]). RC is an integral membrane protein spanning the photosynthetic membrane and composed of three subunits named L, M, and H (left side) whose scaffolding allocates several cofactors (right side, slightly magnified) used to translocate electrons across the phospholipid bilayer. Cofactors are organized in two symmetrical branches (A and B) consisting (from cytoplasm to periplasm) of two ubiquinone-10 molecules (coenzyme Q_{10}, depending to which branch is located are named Q_A, Q_B), a non-heme bivalent iron ion, two bacteriopheophytins (BPh_A, BPh_B) and four bacteriochlorophylls. Two bacteriochlorophylls are present as monomers ($BChl_A$, $BChl_B$) and two forming a functional dimer (D).

This approach enables formation of closed vesicles and protein incorporation simultaneously[16]. Only few examples of protein reconstitution with this method exist. Recently, the Aquaporin-0 was successfully reconstituted by this procedure, using a prolonged (several days) dialysis for detergent removal.[17] Indeed, more studies in protein reconstitution in polymersomes by MVT are required to deepen the knowledge on protein function, orientation and resistance as well on the whole system morphology.

The MVT technique is here proved to be effective in reconstituting the photosynthetic reaction center (RC) in artificial vesicles. Among the different available detergent removal procedures, the size exclusion chromatography was chosen being fast, efficient and simple and not yet applied to polymersomes. The selected protein RC is an integral membrane protein from the red non-sulfur bacterium *Rhodobacter (R.) sphaeroides* which plays a central role in the conversion of solar energy during the photosynthetic process (Figure 1): photon absorption generates a cascade of electron transfer reactions eventually leading to an electron-hole pair sitting on the opposite sites of the protein, 35-40 Å apart.[18]

The final electron acceptor, a quinone molecule sitting in a dedicated binding pocket called Q_B, is a very sensitive internal probe of the outer protein environment, offering a tool to gather direct information on the protein localization in the artificial membrane. On the other hand, RCs are very appealing for biotechnological applications in energy conversion, biosensing and optoelectronics, hence finding a suitable chemical environment in which its function is preserved and in which orientation can be controlled for maximum interaction with the external electrical circuit is crucial.[19-21] Polymersome reconstituted RCs are found to accommodate in the more mobile, less hydrophobic portion of the tri-block copolymer artificial vesicle, namely in the external PMOXA layer, making the RC completely available for interaction with the external environment.

Materials and methods

Chemicals

Reagents were purchased from Sigma-Aldrich or Fluka at the highest commercial quality and used without further purification. Hexane and 2-methyloxazoline were distilled on molecular sieves under nitrogen atmosphere. Acetonitrile and 1,2-dichloroethane (both anhydrous grade) were stored in glove box under N_2 atmosphere. Bis(hydroxyalkyl) terminated poly-(dimethylsiloxane) (PDMS, CAS number 156327-07-0, declared average molecular weight $M_n \approx 5600$ Da) was characterized by ^{1}H-NMR, showing a structure formed by 61

monomer dimethylsiloxane units, corresponding to an actual molecular weight of Mn≈4700 Da (see Figure S5.1).
1-palmitoyl-2-oleoyl-sn-glycero-3-phosphocholine (POPC) was purchased from Avanti Polar Lipids.

Synthesis.

The tri-block copolymers $PMOXA_n$-$PDMS_m$-$PMOXA_n$, was synthesized according to literature[22] as illustrated in scheme S5.1. The effective molar ratio between grafted 2-methyloxazoline (MOXA) and PDMS monomers, was determined by NMR integrals (see paragraph S5 in supporting information), showing a final polymer structure of $PMOXA_{22}$-$PDMS_{61}$-$PMOXA_{22}$ (or $A_{22}B_{61}A_{22}$) The $PMOXA_{22}$ was synthesized according to a previously published protocol[23], as detailed in SI.

Protein extraction and purification

Reaction centers were isolated from *Rhodobacter sphaeroides* strain R26 as previously described.[24] The optical spectrum of the RC was recorded in the range 250 – 1100 nm and the absorbance ratios A_{280}/A_{802} (≤ 1.35) and A_{760}/A_{860} (≤ 1) were used to assess protein purity and integrity, respectively. Activity and quinone content were checked by recording the charge recombination (CR) kinetics by using a kinetic spectrometer of local design described elsewhere.[24] RC concentration was inferred by the scattering corrected absorbance at 802 nm (ε = 288 $mM^{-1}cm^{-1}$).

Preparation of liposomes, polymersomes and PMOXA aggregates.

Liposomes and polymersomes were prepared by the micelle to vesicle transition consisting in removing the detergent from mixed micelles containing phospholipids or organic polymers to induce vesicle formation.[16] In this paper MVT technique was tailored to prepare polymersomes and PMOXA aggregates.
RC-Polymersomes
Stock solution of $A_{22}B_{61}A_{22}$ (14 mM in ethanol) was prepared and kept at -20 °C. Thirty µL aliquots of stock solution were carefully dried under a gentle N_2-stream in a rotating Eppendorf tube, to form a uniform film onto its wall. When needed, quinone pool was obtained by adding 20 µL of decylubiquinone (dQ) of a 1 mM ethanol stock solution. 0.5 mL of 4% (w/v) cholate solution in 5 mM phosphate buffer at pH 7 containing 10 mM KCl is added to the film and mildly sonicated until full dissolution and 12 µL aliquot RC stock solution (84 µM in Tris 10 mM, EDTA 1 mM, LDAO 0.025%, pH 8 buffer) are then added.
Detergent was removed by size exclusion chromatography loading the solution on a 20×1 cm Sephadex G-100 (Pharmacia) column. During elution the detergent monomers, sodium cholate and LDAO, elute slowly while the polymersomes form at the elution front in a ~1 mL band eluting in 2-3 minutes. The RC concentration in the eluate is ~1µM and the final molar ratio ABA/RC/dQ is 420:1:20.
RC-PMOXA MVT-like aggregates
RC-PMOXA aggregates were prepared applying the MVT method using 30 µL aliquot of $PMOXA_{22}$ stock solution (27 mM in ethanol). The final molar ratio PMOXA/RC/dQ was 840:1:20, ensuring an equal molar ratio between the hydrophilic block and the RC as in the ABA cases.
Liposomes
RC containing POPC liposomes were prepared by the same above outlined and previously published MVT techniques.[25] The final POPC/RC/dQ molar ratio was 1000:1:20.
Checking protein reconstitution
To exclude any RC adventitious association with aggregates, size exclusion chromatography based on Sepharose 4B (Pharmacia)[9] was performed on polymersome obtained from G-100 column, or RC-$PMOXA_{22}$ solution and on RC-cholate micelles. The elution profile was obtained by recording 802 nm absorbance of 0.35 mL fractions.

Vesicle characterization

Complete detergent removal in the RC containing eluate fractions was demonstrated by ATR-FTIR recorded with a Varian 670-IR spectrometer, checking the absence of the characteristic asymmetric carboxylate stretching at 1555 cm^{-1} of cholate.[26, 27]
The hydrodynamic radius of the vesicles was assessed by dynamic light scattering (DLS) measurements using Malvern Zetasizer Nano 2590.[25]
AFM vesicle images were obtained in air in tapping mode by using a PSIA XE-100 atomic force microscope equipped with a standard 125 µm long rectangular cantilever with a force constant of 42 N/m and a nominal resonant frequency of 320 kHz. 10 µL of the polymersome suspension ($[A_{22}B_{61}A_{22}] \approx 500$ µM) in MilliQ water were deposited on mica slides, incubated for 3 minutes at room temperature, then rinsed with Milli-Q water and analyzed after drying. Topographic images were analyzed using the software XEI (PSIA Corp., version 1.7.3) and the cross section profiles were obtained.
CryoEM images were obtained from frozen hydrated samples. Samples were prepared by applying a 3 µl aliquot to a previously glow-discharged Quantifoil holey carbon grid (Ted Pella, USA). Before plunging the grid into liquid ethane, the grid was blotted for 1.5 s in a chamber at 4°C and 90% humidity using a FEI Vitrobot Mark IV (FEI company, the Netherlands). The particles were imaged using a Tecnai G2 F20 transmission electron microscope equipped with a Field Emission Gun (FEI company, the Netherlands) operating at an acceleration voltage of 200 kV and recorded at low dose with a 2k x 2k Ultrascan Gatan CCD camera.

Kinetic measurements

Charge recombination (CR) kinetics and protein orientation assay were measured using a kinetic spectrophotometer of local design.[24]
RC orientation within the vesicles was assayed by adding 10 µM reduced horse heart cytochrome c (cyt c) to the investigated solution and the amplitude of the CR signal at 865 nm was compared to that in the absence of cytochrome. [28]

To evaluate RC photocycle rate, a solution containing 1 μM RC – entrapped in $A_{22}B_{61}A_{22}$ polymersomes or in $PMOXA_{22}$ aggregates – and 10 μM reduced cyt c in phosphate buffer at pH 7 was continuously illuminated with a red-filtered light and absorbance change was followed at 551 nm. As electron acceptor the synthetic dQ was employed with a final concentration of 20 μM. dQ was used instead of the native ubiquinone-10 since, while both have an high affinity for the Q_B-site of the RCs,[29] the former is less hydrophobic and can be easily dispersed in the solution from an ethanol stock solution, while the latter, much more hydrophobic, needs to be vehiculated *via* triton X-100 micelles. DecylQuinone was used according to two different experimental settings: in the first configuration, as reported in vesicle preparation protocol, dQ was added in RC-ABA polymersomes or in RC-PMOXA aggregates in the film formation step before the G-100 size exclusion chromatography which removes the not entrapped dQ. In that case, these samples are labeled as "dQ confined", as after reported. In the second case dQ was added after the G-100 column and samples are labeled as "dQ free". Finally, the rate constant of the process was determined as the initial slope divided by the total amplitude of the signal and normalized for the amount of photoactive RC.

Results and discussion

Control of orientation in membrane proteins reconstituted in artificial membrane vesicles is a key issue for the maintenance of their net enzymatic activity. In this work, the formation of polymersomes based on tri-block copolymers by MVT is demonstrated and the actual localization of the RC is shown. Our result, besides the interest in the manipulation of RC for photovoltaics[30-32] and photocatalysis, has a great fundamental interest, eventually showing that it is possible to gain a control on organization and orientation of membrane proteins in polymersomes.

The RC in figure 1, upon photon absorption, promotes one electron sitting on D in its excited state and then it shuttles to the electron acceptors Q_A and finally to Q_B, generating the final charge separated state $D^+Q_B^-$ (or $D^+Q_A^-$ in case the Q_B functionality is inhibited or removed). In the absence of external electron donors, the charge recombination reaction $D^+Q_B^- \rightarrow DQ_B$ or $D^+Q_A^- \rightarrow DQ_A$ occurs, with typical kinetic constants of 1 and 10 s^{-1}, respectively. Conversely, in the presence of external electron donors the oxidized D^+ is re-reduced and a second photon impinges a second electron so that the final quinone Q_B, now doubly reduced, is doubly protonated and it is released as quinol. The Q_B-functionality can be hence restored by a new quinone uptaken from an exogenous pool.[33] This photocycle can be reconstituted in solution and driven as long as the exogenous pools of external electron donor (cytochrome) or quinone become exhausted.[34] Cytochrome c_2 is the physiological electron donor to the oxidized special pair, but in isolated protein it can be replaced by horse hearth cytochrome c.

The actual reconstitution of the RC is accomplished during the formation of the closed vesicle, using the MVT method which is widely applied in reconstituting membrane proteins in liposomes. This technique has the advantage of being very mild and is accompanied by a high reconstitution yield of fully functional proteins. The successful polymersomes formation and RC reconstitution are demonstrated by several independent experiments below described.

RC reconstitution protocol starts with a mixed micelles solution containing sodium cholate and the polymer. Figure 2 shows the ATR-FTIR spectra of starting solution (mixed micelles), of the final eluate ($A_{22}B_{61}A_{22}$ polymersomes) from Sephadex G-100 column along with pure sodium cholate and pure $A_{22}B_{61}A_{22}$ as comparison. The typical asymmetric carboxylate stretching peak at 1555 cm^{-1} detectable in the sodium cholate and mixed micelles solutions (traces b and c) is absent in the polymersome solution (trace d), where only the ABA signals, mainly arising from $Si–CH_3$ stretching at 1260 cm^{-1} and amide C=O stretching at 1635 cm^{-1} (trace a), are present.

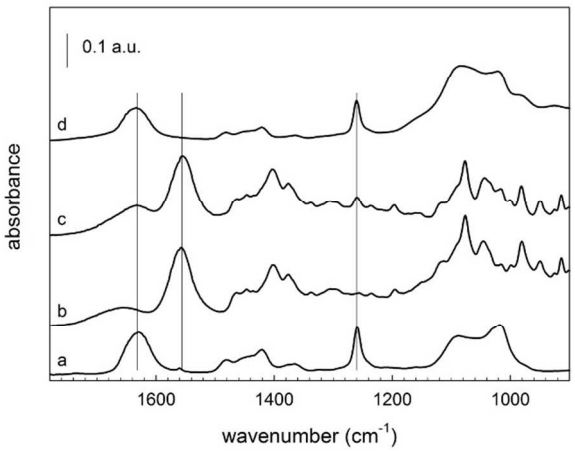

Figure 2. ATR-FTIR spectra of (a) $A_{22}B_{61}A_{22}$ as pure compound, (b) 4% sodium cholate solution in phosphate buffer, (c) $A_{22}B_{61}A_{22}$ – sodium cholate mixed micelle solution and (d) $A_{22}B_{61}A_{22}$ polymersomes solution obtained as eluate of the Sephadex G-100 column. Peak attribution in $A_{22}B_{61}A_{22}$: 1020 and 1091 cm^{-1} Si–O–Si stretching; 1260 cm^{-1} $Si–CH_3$ stretching; 1635 cm^{-1} amide C=O stretching.

The actual protein reconstitution must be demonstrated in the case of artificial membrane and RC to rule out any adventitious aggregation between protein and vesicles. Direct evidences from the RC photochemical behavior (see below), indicates protein incorporation; further evidence was obtained by chromatographic experiments. Size exclusion chromatography has the advantage of being a fast technique to obtain closed vesicles[13] of amphiphilic molecules. Sephadex G-100 is a dextran based size exclusion chromatography medium suitable for liposome reconstitution,[16] but never employed so far for polymersomes. To check whether such medium is suitable also for artificial membrane, polymersomes obtained from G-100 chromatography were subjected to a further step with Sepharose 4B, an agarose based size exclusion

chromatography, widely used to separate closed vesicles from any non-incorporated protein.[9, 35, 36]

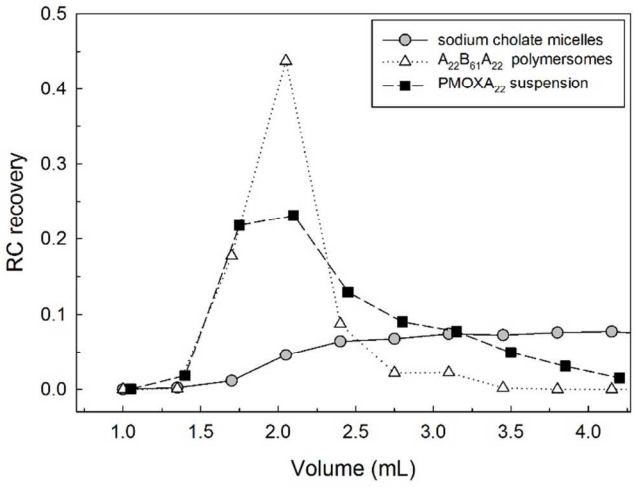

Figure 3. Elution profile on Sepharose 4B of RC-$A_{22}B_{61}A_{22}$ polymersomes (empty triangles) and of RC-$PMOXA_{22}$ aggregates (black squares). As comparison, the elution profile of RC-cholate micelles is also shown (grey circle). Recovered RC is calculated as the fraction found in each aliquot over the total loaded protein. RC quantification is obtained from bacteriochlorophyll dimer absorption band at 802 nm.

Figure 3 shows that RC elutes very slowly in cholate micelles, being depleted of its solubilizing detergent; on the opposite, the elution of RC in polymersomes from the Sephadex G-100 step takes place in a single sharp peak, with very small free RC amounts emerging in the following aliquots. This result clearly indicates that the fraction of incorporated RC in polymersomes is 0.75±0.05 of the total loaded protein. A third elution profile for RC-PMOXA solution has been recorded. In this case RC elutes in a single peak indicating that PMOXA molecules always surround the protein. The presence of a single broad peak do not imply that PMOXA forms large aggregates by itself, but rather that the protein tends to surround its own hydrophobic portion with the PMOXA molecules available in solution, similarly to the behavior of the detergents (LDAO o Triton-X100) generally used with membrane protein solutions. In PMOXA a recovery of 0.60±0.05 was found. The aggregates have variable sizes, the largest ones elute rapidly while the smaller ones are delayed. The RC is reconstituted in both polymersomes (obtained with Spehadex G-100) and PMOXA aggregates, hence the use of Sepharose 4B was omitted in the reconstitution procedure.

As mentioned, a further confirmation of the actual reconstitution of the protein is given by the charge recombination reaction which takes place once the RC has been excited by a light pulse to form a charge separated state. In absence of exogenous quinone, the electron can reach the acceptor system and reduce the two quinones Q_A and Q_B (Figure 1). The final states recombine with the optical decay profile showing a bi-exponential trace with a fast and slow time constants associated to $D^+Q_A^-$ and $D^+Q_B^-$ respectively.

The time constant k_S of the CR reaction from the $D^+Q_B^-$ state is very sensitive to the environment in which the protein is allocated: the higher is the difference in the energy levels between the semiquinones Q_A^- and Q_B^-, the slower is the recombination rate.[37] k_S varies from roughly 1 s^{-1} in LDAO,[24] to 0.44 s^{-1} in POPC liposomes to 0.3 s^{-1} in phosphatidylglycerol liposomes.[28] The RC incorporated in ABA polymersomes shows a k_S of 1.70±0.05 s^{-1} faster than in the detergent medium, indicating that, upon reconstitution, the environment changes from the initial mixed micelle to the polymersome, resulting in a smaller energy level difference of the semiquinones (Figure 4).

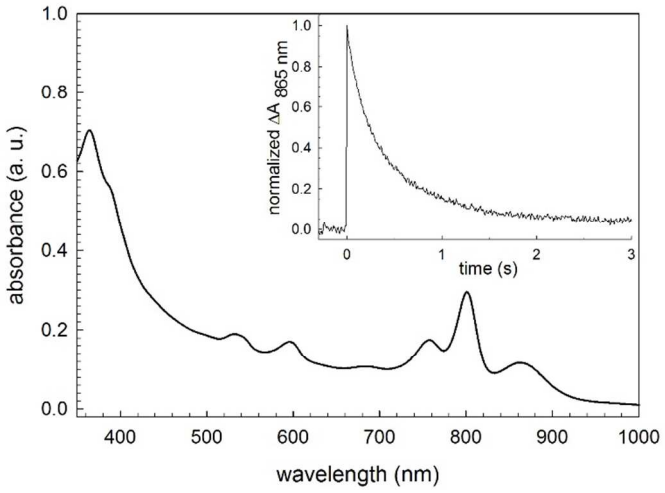

Figure 4. Optical spectrum of the RC reconstituted polymersome. The NIR peaks at 760, 802, and 865 nm are the protein fingerprints (see material and methods). The baseline of the spectrum is deformed by the light scattering due to polymersomes. In the inset is shown the normalized absorption trace for the charge recombination reaction recorded at 865 nm.

Interestingly, the ability of generating a charge separated state, from which eventually recombination takes place, demonstrates the functional integrity of the RC and its structural integrity as shown by the optical Vis-NIR spectrum (Figure 4). Furthermore the Q_B functionality can be fully inhibited by the addition of the well-known herbicide terbutryn in the reconstituted system (see figure S1.1 in supporting information).

Polymersome morphology was characterized by cryo-EM, AFM and DLS. Cryo-EM images were obtained for the polymersomes obtained by MVT method in absence of any salt and showed the presence of closed unilamellar vesicles with an average diameter of 103±30 nm from the direct observation of 11 individual vesicles (Figure 5 right). Membrane thickness was found 5±1 nm in agreement with Choi et al.[38] A further indication of formation of closed vesicles is the successful entrapment of the hydrophilic dye pyranine within the internal aqueous core of the polymersomes reconstituted with the RC (see figure S2.1 in supporting information).[13]

Journal Name RSCPublishing

ARTICLE

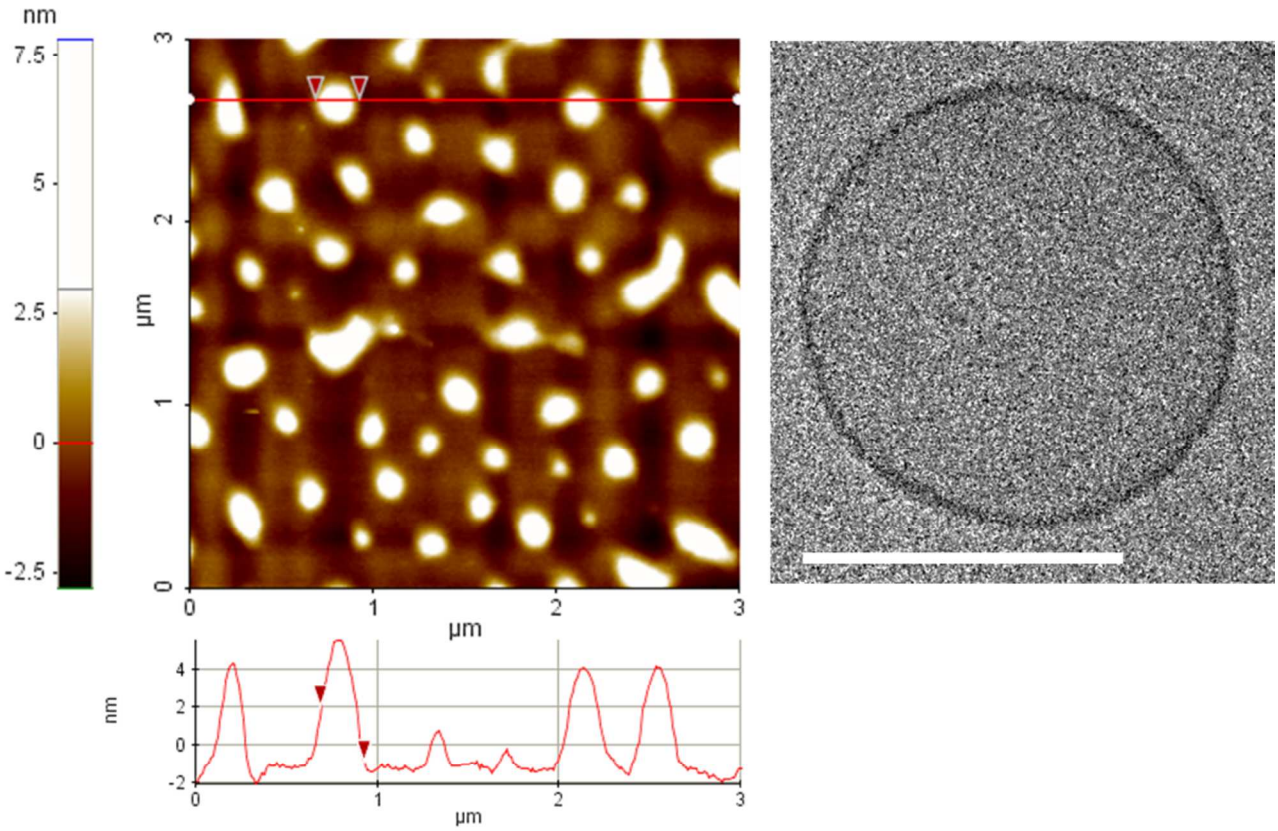

Figure 5. Left: AFM image of ABA polymersomes showing several spheres of about 100 nm plus smaller structures. Right: cryo-EM micrograph of polymersomes prepared in milliQ water. Scale bar: 100 nm.

AFM (Figure 5, left panel) also showed a large number of vesicles close to 100 nm are accompanied by some smaller circular structures. ABA-polymersomes were also analyzed by dynamic light scattering. An average polymersome hydrodynamic diameter of 130±30 nm was found regardless of the RC incorporation, oppositely to our experience with liposomes where decreasing the POPC:RC ratio produces larger liposomes (see Figure S3.1).[25]

This result suggests two possible scenarios: *i)* the RC is packed in the most hydrophobic portion of the ABA, *i.e.* the PDMS which mimics the bilayer, but the packing interaction has no effect on the size of the vesicle. *ii)* The RC is trapped in the less hydrophobic and less rigid environment, the PMOXA, which constitutes the palisade between the hydrophobic layer and the aqueous solution. This second possibility was easily checked by recording the charge recombination reaction traces in the RC-PMOXA aggregates, obtained by gel exclusion chromatography. An exogenous quinone – decylquinone (dQ) – was added to this aggregate to neglect CR contribution coming from $Q_{A,}$ focusing the attention on the more sensitive Q_B site. For comparison, the RC reconstitution with excess dQ was also done with ABA-polymersome and CR was measured. The k_S values obtained for RC-PMOXA and ABA-polymersome were found 1.95±0.05 s^{-1} and 1.88±0.05 s^{-1} respectively. It should be noted that these values are slightly different from those obtained in the absence of exogenous quinone (1.70±0.05 s^{-1}) as in the latter case the final electron acceptor is the native quinone, the ubiquinone-10, slightly different form dQ. Moreover these k_S can be compared to 0.98±0.05 s^{-1} obtained under the same conditions (i.e. dQ as exogenous quinone) in RC-POPC liposomes, where the protein is firmly packed in the hydrophobic portion of the phospholipid bilayer. In the artificial aggregates the Q_B^- appears to be less stable than in the hydrophobic portion of liposome.

The intriguing hypothesis that the RC may accumulate in the PMOXA portion of the polymersome had to be further confirmed. In the absence of any driving force, as in the MVT technique, no preferential orientation during the RC reconstitution could be in principle expected, in analogy to what happens in RC-POPC liposomes which show a 50:50 distribution of the two possible orientations. In liposomes this can be easily checked by adding a suitable excess of the reduced form of cytochrome c (cyt c^{2+}) to the preformed vesicle. Indeed at pH 7 this 12.5 kDa globular protein is strongly positively charged[28] and it cannot cross the phospholipid bilayer, remaining confined in the external aqueous solution. Cyt c^{2+} will only be able to reduce the oxidized dimers facing toward the exterior of the vesicle, while the portion facing the interior of the vesicle will be unaffected by cyt c^{2+}. This is a straightforward experiment since the electron donation time of cyt c^{2+} to the dimer is in the order of few microseconds, thousand time faster than k_S, hence on the seconds time scale the RC reduced by cytochrome will be silent, while those wrongly oriented will maintain their normal CR reaction time. This is clearly shown in figure 6 where the addition of cyt c^{2+} halves the amplitude of the signal, but the CR reaction of un-reduced RC is unchanged.

On the contrary, in RC-polymersomes the interaction with cyt c^{2+} fully reduces the oxidized dimer and, accordingly the CR signal disappears, only a small fast contribution remaining visible. It can be concluded that all RCs are exposed to the bulk solution. Interestingly, and again oppositely to liposomes, the small optical signal appearing after the light flash is due to the electron donation time from cyt to RC, which appears to be much slower in polymersomes, suggesting somehow an hindered diffusion of the heme protein trough the PMOXA palisade.

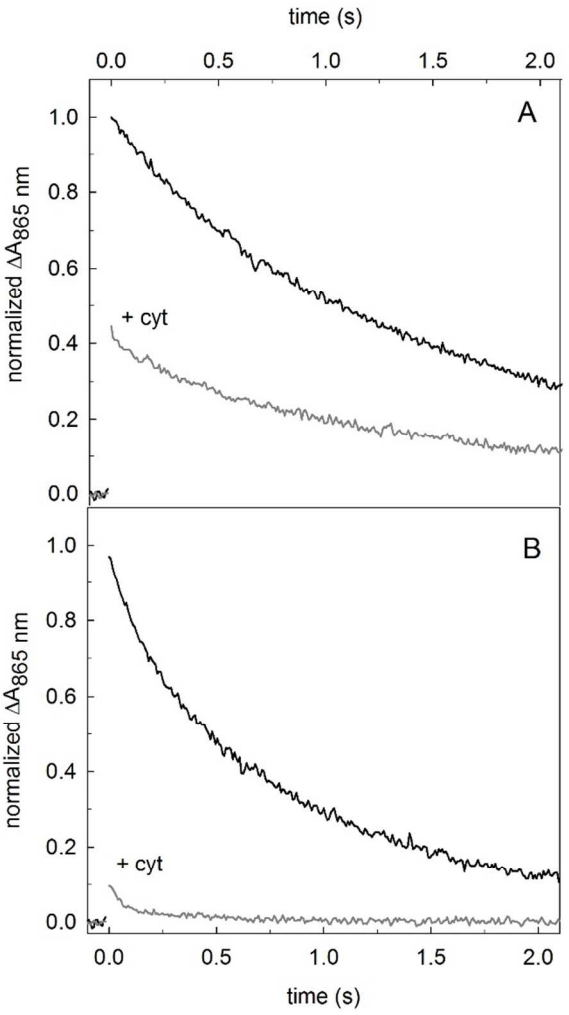

Figure 6. Normalized charge recombination kinetics of 1 μM RC in POPC liposome (fig. A) and ABA polymersomes (fig. B) in absence (black line) or in presence (gray line) of 10 μM reduced cytochrome c in phosphate buffer, KCl 10 mM at pH 7.

The reduction of the oxidized dimer can also be investigated under continuous illumination, exploiting the photocycle that transfers electrons from cytochrome to quinone.

The photocycle was run on both RC-polymersomes and RC-PMOXA aggregates under two different conditions, one in which the exogenous quinone is confined into these systems and a second in which it is freely distributed in all the compartments, including the bulk solution (Figure S4.1 and S4.2). As described earlier, the photocycle will maintain its turnover until either the cytochrome or the quinone pool become exhausted. Comparison between different conditions based on the photocycle rate are reliable only when the concentration of the two pools are larger than that of the protein, hence in the initial part of the experiment. Both conditions rely on the use of gel exclusion chromatography, which ensures that any free dQ is separated from the systems.

The photocycle rate, normalized to the photoactive RC concentration, in the confined condition was found twice faster in RC-PMOXA than in RC-polymersomes (0.56±0.01 s^{-1} vs

0.28±0.01 s^{-1}). The same photocycle was performed in free dQ condition, in which dQ is added in the bulk solution once the aggregate have formed: RC-PMOXA aggregates and RC-polymersomes have an almost identical normalized rate of 0.64±0.01 s^{-1} and 0.59±0.01 s^{-1}. Both in RC-polymersomes and in RC-PMOXA aggregates, the free quinone condition results in a faster photocycle rate (Table 1), and this increase can be taken as a qualitative parameter for quinone accessibility to the Q_B binding site.

	Photocycle rate (s^{-1})	Photocycle rate (s^{-1})
	Confined dQ	Free dQ
Polymersomes	0.28±0.01	0.59±0.01
RC-PMOXA	0.56±0.01	0.64±0.01
RC-POPC liposomes	1.18±0.01	0.91±0.01
RC-POPC liposomes	1.23±0.01*	0.90±0.01

*confined quinone = UQ_{10}

Table 1. Photocycle rate measured by following cytochrome oxidation reaction in presence of embedded RC in $A_{22}B_{61}A_{22}$ polymersomes, in RC-PMOXA aggregates and in lipid POPC liposomes.

The ratio is close to 2 in polymersomes and roughly 1.1 in RC-PMOXA, indicating that it is much harder for quinones confined in the polymersome's hydrophobic core to reach the protein's binding site than for the quinone confined in the RC-PMOXA aggregates. This in turn suggests that in the RC-polymersomes the RC is located far from the PDMS core and most likely embedded in the PMOXA palisade. Moreover, the rate similarity between the free dQ cases implies that the dQ externally added to polymersomes dissolves in the PMOXA moiety without further diffusing in the PDMS region.

To gain insight in the Q_B site accessibility, POPC liposomes under the same free and confined quinone conditions were also prepared, using either dQ or UQ_{10} as confined quinone and dQ as free quinone. In this case the observed photocycle rates for free and confined quinone, normalized for the photoactive and correctly oriented RC, show that the confined quinone works better than the free one as expected for the RC correctly embedded in the vesicle bilayer and with the membrane-dispersed UQ_{10} in close proximity to the Q_B-site. This result indicates that the free/confined quinone comparison effectively unveils the efficiency of communication between the Q_B-site and its environment.

The results gathered on the reconstituted systems show that the photosynthetic RC is reconstituted within the artificial membrane allocating itself in the palisade formed by the hydrophilic PMOXA moiety rather than in the more hydrophobic PDMS region. An attempt to reconstitute the RC in a tri-block copolymer with a shorter PMOXA block, namely $A_{10}B_{61}A_{10}$, was not successful since no polymersome were obtained by MVT, probably because the PMOXA moiety is too short for aggregation. The MVT techniques, based on the data here presented, seems to favor the reconstitution of the protein solely in the external palisade, while the PMOXA moiety facing the core of the polymersome seems unable to accommodate any protein. This "selectiveness" may result from the actual dimension of the closed vesicles, whose internal lumen is very densely packed by the PMOXA polymers, making the aqueous internal core hindered to accommodate the 100 kDa protein.

Polymersomes were lastly checked for their stability and ability to preserve RC functionality over time. The sample turbidity at 650 nm, indicative of the presence of light scatterers, and the absorption ratio at A_{802}/A_{765}, indicative of the protein integrity in solution were monitored. These two data were collected, for comparison, also in the case of liposomes and although the stability of the protein results unchanged in the two cases, polymersomes show a much smaller tendency to aggregate, as the turbidity remains constant, oppositely to what happens in the model membrane (Figure 7).

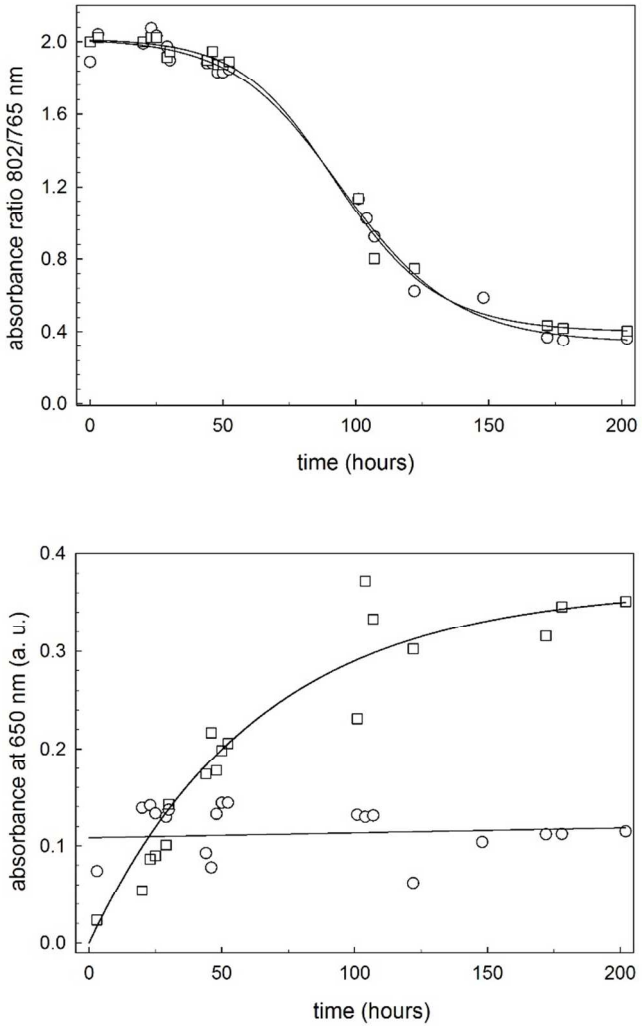

Figure 7. ABA artificial vs POPC model membranes. Time evolution of RC integrity (upper panel) and vesicle aggregation (bottom panel) in polymersomes (circles) and liposomes (squares). Experiments performed in ambient light condition.

Conclusions

Polymersomes formation and fully active reaction center reconstitution were successfully obtained by optimizing the micelle-to-vesicle transition technique to $PMOXA_{22}$-$PDMS_{61}$-$PMOXA_{22}$ tri-block copolymers. To our knowledge this is the first attempt to adapt this technique to artificial membranes. The use of MVT appears to asymmetrically reconstitute the protein in the less hydrophobic region formed by the $PMOXA_{22}$, confining the photosynthetic reaction center exclusively in the part facing the bulk water solution. MVT using size exclusion chromatography is furthermore a very convenient technique to use in assembly of polymersomes containing proteins as it is faster and less material consuming than dialysis, still maintaining small and monodisperse closed vesicles.

Interestingly, polymersomes and liposomes show the same behavior in preserving the RC functionality, fully active for more than 50 hours under ambient light condition, but the artificial membrane show a much longer stability in comparison to model membranes.

These artificial closed vesicles hence represent an interesting building block in the assembly of supramolecular aggregates to be used in energy conversion machineries based on organic-biological hybrids photosynthetic systems.

Acknowledgements

JH acknowledges the University of Namur and the Erasmus Program for financing a scientific visit to the University of Bari.

Dr. Adriana Trapani is warmly acknowledged for DLS measurements and data discussion.

This work was financially supported by Ministero dell'Istruzione, dell'Università e della Ricerca (MIUR), Research Project of National Interest (prot. 2010C4R8M8); Regione Puglia "Progetti Reti di Laboratori Pubblici di Ricerca WAFITECH Prog. Cod. 09, Sens&MicroLAB Prog. Cod. 15 and e PHOEBUS Prog. Cod. 31; MIUR and DiTECH (PON 02_00563_3316357 Molecular Nanotechnology for Health and Environment MAAT).

Notes and references

[a] Chemistry Department, Università degli Studi di Bari "Aldo Moro", via Orabona 4, 70125 Bari - Italy

[b] CNR-IPCF, Istituto per i processi Chimico-Fisici, UOS Bari (Italy). via Orabona 4, 70125 Bari – Italy. e-mail: massimo.trotta@cnr.it

[c] CNR-ICCOM, Istituto di Chimica dei Composti Organometallici, via Orabona 4, 70125 Bari – Italy.

[d] Chemistry Department and Namur Research College (NARC), University of Namur (UNamur), Rue de Bruxelles 61, Namur, Belgium.

[e] Electron Microscopy Lab, Nanochemistry Department Istituto Italiano di Tecnologia (IIT) Via Morego 30, 16163 Genova – Italy.

[f] King Abdullah University of Science and Technology, Biological and Environmental Sciences and Engineering Division, 23955-6900, Thuwal Kingdom of Saudi Arabia.

1. A. G. Lee, *Bba-Biomembranes*, 2004, **1666**, 62-87.
2. D. E. Discher and A. Eisenberg, *Science*, 2002, **297**, 967-973.
3. Y.-H. M. Chan and S. G. Boxer, *Current Opinion in Chemical Biology*, 2007, **11**, 581-587.
4. M. M. Parmar, K. Edwards and T. D. Madden, *Bba-Biomembranes*, 1999, **1421**, 77-90.
5. M. Antonietti and S. Forster, *Adv Mater*, 2003, **15**, 1323-1333.
6. M. Kumar, M. Grzelakowski, J. Zilles, M. Clark and W. Meier, *Proceedings of the National Academy of Sciences of the United States of America*, 2007, **104**, 20719-20724.
7. A. Graff, M. Sauer, P. Van Gelder and W. Meier, *Proceedings of the National Academy of Sciences of the United States of America*, 2002, **99**, 5064-5068.
8. H. J. Choi and C. D. Montemagno, *Nano Lett*, 2005, **5**, 2538-2542.
9. A. Graff, C. Fraysse-Ailhas, C. G. Palivan, M. Grzelakowski, T. Friedrich, C. Vebert, G. Gescheidt and W. Meier, *Macromolecular Chemistry and Physics*, 2010, **211**, 229-238.
10. C. Nardin, J. Widmer, M. Winterhalter and W. Meier, *The European Physical Journal E*, 2001, **4**, 403-410.
11. K. Kitatokarczyk, J. Grumelard, T. Haefele, W. Meier and K. Kita-Tokarczyk, *Polymer*, 2005, **46**, 3540-3563.
12. H. J. Choi, J. Germain and C. D. Montemagno, *Nanotechnology*, 2006, **17**, 1825-1830.
13. F. Milano, M. Trotta, M. Dorogi, B. Fischer, L. Giotta, A. Agostiano, P. Maroti, L. Kalman and L. Nagy, *J Bioenerg Biomembr*, 2012, **44**, 373-384.
14. H. R. Marsden, C. B. Quer, E. Y. Sanchez, L. Gabrielli, W. Jiskoot and A. Kros, *Biomacromolecules*, 2010, **11**, 833-838.
15. J. Koepke, E.-M. Krammer, A. R. Klingen, P. Sebban, G. M. Ullmann and G. Fritzsch, *J Mol Biol*, 2007, **371**, 396-409.
16. M. Ollivon, S. Lesieur, C. Grabielle-Madelmont and M. Paternostre, *Bba-Biomembranes*, 2000, **1508**, 34-50.
17. M. Kumar, J. E. Habel, Y. X. Shen, W. P. Meier and T. Walz, *J Am Chem Soc*, 2012, **134**, 18631-18637.
18. P. Maróti and M. Trotta, in *CRC Handbook of Organic Photochemistry and Photobiology, Third Edition - Two Volume Set*, CRC Press, 2012, DOI: doi:10.1201/b12252-56, pp. 1289-1324.
19. Y. Kim, S. A. Shin, J. Lee, K. D. Yang and K. T. Nam, *Nanotechnology*, 2014, **25**, 342001.
20. L. Nagy, M. Magyar, T. Szabo, K. Hajdu, L. Giotta, M. Dorogi and F. Milano, *Curr. Protein Peptide Sci.*, 2014, **15**, 363-373.
21. O. Yehezkeli, R. Tel-Vered, D. Michaeli, I. Willner and R. Nechushtai, *Photosynth Res*, 2014, **120**, 71-85.
22. C. Nardin, T. Hirt, J. Leukel and W. Meier, *Langmuir*, 2000, **16**, 1035-1041.
23. F. Wiesbrock, R. Hoogenboom, M. a. M. Leenen, M. a. R. Meier and U. S. Schubert, *Macromolecules*, 2005, **38**, 5025-5034.
24. A. Agostiano, F. Milano and M. Trotta, *Eur J Biochem*, 1999, **262**, 358-364.
25. F. Milano, F. Italiano, A. Agostiano and M. Trotta, *Photosynth Res*, 2009, **100**, 107-112.
26. L. Giotta, D. Mastrogiacomo, F. Italiano, F. Milano, A. Agostiano, K. Nagy, L. Valli and M. Trotta, *Langmuir*, 2011, **27**, 3762-3773.
27. V. De Leo, L. Catucci, A. Falqui, R. Marotta, M. Striccoli, A. Agostiano, R. Comparelli and F. Milano, *Langmuir*, 2014, **30**, 1599-1608.
28. L. Nagy, F. Milano, M. Dorogi, A. Agostiano, G. Laczko, K. Szebenyi, G. Varo, M. Trotta and P. Maroti, *Biochemistry-Us*, 2004, **43**, 12913-12923.
29. J. C. McComb, R. R. Stein and C. A. Wraight, *Biochim Biophys Acta*, 1990, **1015**, 156-171.
30. R. R. Tangorra, A. Antonucci, F. Milano, S. la Gatta, A. Operamolla, R. Ragni, A. Agostiano, M. Trotta and G. M. Farinola, *MRS Online Proceedings Library*, 2015, **1722**.
31. R. Ragni, O. H. Omar, R. R. Tangorra, F. Milano, D. Vona, A. Operamolla, S. La Gatta, A. Agostiano, M. Trotta and G. M. Farinola, *MRS Online Proceedings Library*, 2014, **1689**.
32. F. Milano, R. R. Tangorra, O. Hassan Omar, R. Ragni, A. Operamolla, A. Agostiano, G. M. Farinola and M. Trotta, *Angewandte Chemie*, 2012, **124**, 11181-11185.
33. G. Feher, J. P. Allen, M. Y. Okamura and D. C. Rees, *Nature*, 1989, **339**, 111-116.

34. F. Milano, L. Gerencser, A. Agostiano, L. Nagy, M. Trotta and P. Maroti, *J Phys Chem B*, 2007, **111**, 4261-4270.
35. A. Graff, M. Sauer, P. Van Gelder and W. Meier, *Proceedings of the National Academy of Sciences*, 2002, **99**, 5064-5068.
36. M. Kumar, M. Grzelakowski, J. Zilles, M. Clark and W. Meier, *Proceedings of the National Academy of Sciences*, 2007, **104**, 20719-20724.
37. F. Milano, A. Agostiano, F. Mavelli and M. Trotta, *Eur J Biochem*, 2003, **270**, 4595-4605.
38. H. J. Choi, E. Brooks and C. D. Montemagno, *Nanotechnology*, 2005, **16**, S143-S149.

Electronic Supplementary Information (ESI) available: Synthesis ABA details and supplementary figures reported. See DOI: 10.1039/b000000x/

